Computer Modeling in Engineering & Sciences CMES, vol.122, no.2, pp.571-591, 2020

Beam Approximation for Dynamic Analysis of Launch Vehicles Modelled as Stiffened Cylindrical Shells

Siyang Piao[1], Huajiang Ouyang[1, 2] and Yahui Zhang[1, *]

Abstract: A beam approximation method for dynamic analysis of launch vehicles modelled as stiffened cylindrical shells is proposed. Firstly, an initial beam model of the stiffened cylindrical shell is established based on the cross-sectional area equivalence principle that represents the shell skin and its longitudinal ribs as a beam with annular cross-section, and the circumferential ribs as lumped masses at the nodes of the beam elements. Then, a fine finite element model (FE model) of the stiffened cylindrical shell is constructed and a modal analysis is carried out. Finally, the initial beam model is improved through model updating against the natural frequencies and mode shapes of the fine FE model of the shell. To facilitate the comparison between the mode shapes of the fine FE model of the stiffened shell and the equivalent beam model, a weighted nodal displacement coupling relationship is introduced. To prevent the design parameters used in model updating from converging to incorrect values, a pre-model updating procedure is added before the proper model updating. The results of two examples demonstrate that the beam approximation method presented in this paper can build equivalent beam models of stiffened cylindrical shells which can reflect the global longitudinal, lateral and torsional vibration characteristics very well in terms of the natural frequencies.

Keywords: Finite element method, model updating, stiffened shell, beam approximation, model reduction.

1 Introduction

A stiffened cylindrical shell consists of skins and ribs with high specific stiffness and specific strength and is widely used as the main load-bearing body of a launch vehicle [Davila, Bisagni and Rose (2015); Hao, Wang, Tian et al. (2016); Hilburger, Lindell, Waters et al. (2017); Wang, Tian, Hao et al. (2016)]. To minimise the scale of computational models in load calculation, control, dynamic analysis, stability analysis, etc., launch vehicles are often reduced to equivalent simple models [Grimes, Mc Tigue, Riley et al. (1970); Nurre, Ryan, Scofield et al. (1984); Pinson (1970); Zipfel (2014)] which should reflect their global longitudinal, lateral and torsional vibration characteristics. The local vibration characteristics are usually considered in a simple manner in the above analysis.

[1] State Key Laboratory of Structural Analysis for Industrial Equipment, Department of Engineering Mechanics, International Center for Computational Mechanics, Dalian University of Technology, Dalian, China.

[2] School of Engineering, University of Liverpool, Liverpool, UK.

[*] Corresponding Author: Yahui Zhang. Email: zhangyh@dlut.edu.cn.

Received: 13 October 2019; Accepted: 29 November 2019.

Since the slenderness ratios of launch vehicles are large, the stiffened cylindrical shells in launch vehicles are usually modelled as beams or spring-mass oscillators [Zipfel (2014)], and the on-board equipment is simplified as lumped masses. The key to a successful reduced model of a launch vehicle is the appropriate treatment of the stiffened cylindrical shell. There is a strong motivation to model the stiffened shell as a beam which can accurately reflect the global longitudinal, lateral and torsional vibration characteristics.

In order to predict the mechanical behaviour of a large complex structure accurately, it is necessary to establish a large-scale fine finite element model (FE model). This is often the case in static analysis as it does not take much time to do this. In dynamic analysis, however, a large-scale fine FE model presents a significant impact on computation time, particularly when optimization, control, or other theoretical work is also required. So reducing the scale of the model without losing the required accuracy is a way forward. In recent decades, model reduction theory [Afonso, Lyra, Albuquerque et al. (2010); Benfield and Hruda (1971); Box and Wilson (1951); Cortex and Vapnik (1995); Craig and Bampton (1968); Friswell, Garvey and Penny (1995); Guyan (1965); Hajela and Berke (1992); Hou (1969); Kaintura, Spina, Couckuyt et al. (2017); Koutsovasilis and Beitelschmidt (2008); Kuhar and Stahle (1974); Matheron (1963); Samuel, Ferranti, Knockaert et al. (2016); Wilson (1974); Wilson, Yuan and Dickens (1982)] has been developed and widely used. It has become an important part of the dynamic analysis of large and complex structures. One methodology is to reduce the mass, stiffness and damping matrices of the FE model by mapping the nodal displacements of the original model to the vector space of the reduction basis. The common methods in this category includes Guyan method [Guyan (1965)], Kuhar method [Kuhar and Stahle (1974)], improved reduction system method [Friswell, Garvey and Penny (1995)], Ritz method [Wilson, Yuan and Dickens (1982)], modal synthesis method [Benfield and Hruda (1971); Craig and Bampton (1968); Hou (1969)], etc. These methods can significantly reduce the scale of a FE model. The accuracy of the reduced model depends on the composition of the reduced basis. Another methodology is the proxy or surrogate model technique, which uses a mathematical expression with a small amount of computation to represent the original model for specific analysis. The commonly used proxy models are the response surface model [Box and Wilson (1951)], Kriging model [Kaintura, Spina, Couckuyt et al. (2017); Matheron (1963)], artificial neural network model [Hajela and Berke (1992)], support vector machine model [Cortex and Vapnik (1995)], etc. Proxy models are established by repeated reanalysis of the original model on a series of sample points and the established reduced model usually lacks physical connections with the original physical parameters. The accuracy of a proxy model depends on the number of sample points and their distribution. It is usually very time-consuming to establish a proxy model of a complex structure with high nonlinearity.

To reduce the scale of the computational models of stiffened cylindrical shells, Cheng and his group [Cai, Xu and Cheng (2014); Cheng, Cai and Xu (2013)] developed a homogenization method and applied it to a three-dimensional periodic structure. Firstly, the complex three-dimensional periodic structure was divided into numerous typical unit cells. Then each typical unit cell was simplified to an equivalent structure with similar stiffness characteristics according to the mechanical properties of each cell. Finally, all the unit cells are replaced by those simple structures. And Hao et al. [Hao, Wang, Tian et al. (2017); Wang, Tian, Hao et al. (2016); Wang, Tian, Zheng et al. (2017)] developed an efficient

equivalent analysis model of stiffened shells to facilitate the post-buckling optimization based on the numerical implementation of asymptotic homogenization method. This kind of methods is suitable for periodic structures with the same unit cells. The difficulty lies in the equivalence of the unit cells. The accuracy is dependent on the understanding of the mechanical properties of the typical unit cells.

The method proposed by Zheng et al. [Wang, Cheng and Li (2013)] divided a FE model of a stiffened cylindrical shell into several regions and assumed that each region was a rigid body. Then, a transformation relationship between the local motion and the global motion was constructed to reduce the FE model. To improve the accuracy of the reduced model, a deformation correction was introduced. Cheng et al. [Cheng and Wang (2014)] extended Zheng and Ding's method and reduced the stiffened cylindrical shell to a super-beam. To improve the accuracy of the super-beam model, three shear coefficients were introduced. This method maintains a good conversion relationship between the super-beam model and the original FE model. The accuracy of the super-beam is good. However, as the super-beam model lacks an obvious physical meaning, it is difficult to establish directly an intuitive finite beam element model for the shell. On the basis of this method, Wang et al. [Wang, Li, Hao et al. (2017); Li, Wang and Cheng (2017)] established a reduced-order model for the structural dynamic analysis of complicated beam-type structure by using a novel reduction basis along with the polynomial interpolation function. The basic idea was to convert the displacements of finite element model nodes in each cross section to a small set of nodes with a few generalized degrees of freedom. Li et al. [Li, Hao, Wang et al. (2019)] presented a model-reduction method based on the proper orthogonal decomposition technique. The basic idea was to extract the principal component of correlation matrix assembled by the nodal displacement field of full-order models subjected to different cross-sectional loads as the transformation matrix.

Pan et al. [Pan, Wang, Ma et al. (2014)] compared the simplified models obtained from several equivalence principles, and proposed a cross-sectional area equivalence principle. After studying the cause for the incorrect increase in torsional stiffness, they obtained a correction coefficient to modify the torsional stiffness of the simplified model established through a cross-sectional area equivalence principle. That method can directly establish an equivalent beam model according to the geometry of the original structure, but it is difficult to take into account the influences of the circumferential ribs and the internal components of the structure. A good accuracy can be obtained only if the cross-sectional moment of inertia of the equivalent beam is close to that of the original structure.

This paper proposes a new beam approximation method for dynamic analysis of launch vehicles modelled as stiffened cylindrical shells. The flow chart of the method is shown in Fig. 1. An initial beam model of the stiffened cylindrical shell is built based on a cross-sectional area equivalence principle and improved through model updating against the modal analysis results of the shell. First, an improvement has been made to the cross-sectional area equivalence principle, the circumferential ribs are considered as lumped masses at the nodes of the beam elements, and so the mass distribution of the initial beam model is much closer to that of the shell along the longitudinal direction. Then, model updating, generally, which is implemented to minimise the difference between model predictions and corresponding test results [Friswell and Mottershead (1995); Mottershead

and Friswell (1993); Mottershead, Link and Friswell (2011)], is utilized to improve the accuracy of the equivalent beam model in this paper, and the iterative model updating method using modal data is selected. During the model updating process, because of the great difference between a beam and a stiffened cylindrical shell, two problems arise: a) the comparison of mode shapes is difficult; b) the design parameters used in model updating are prone to converging to incorrect values. By introducing a weighted nodal displacement coupling relationship, problem a) has been solved. The mode shapes of stiffened cylindrical shell are transformed into the displacements of a series of nodes located on the longitudinal axis of the shell. For problem b), a pre-model updating procedure is added before the proper model updating.

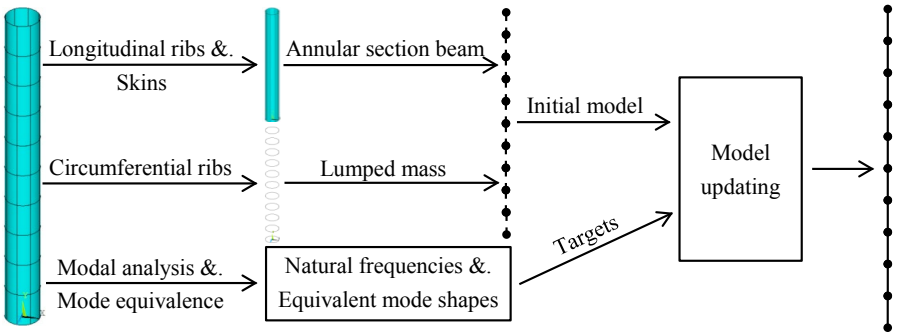

Figure 1: The flow chart of the beam approximation method

The contents of this paper are arranged as follows: The cross-sectional area equivalence principle, the weighted nodal displacement coupling relationship, and the iterative model updating method using modal data are established or discussed in the second to fourth sections. In the fifth Section, an outline of modelling and updating the initial beam is presented. Two examples are given in the sixth section. And some conclusions are drawn in the last Section.

2 Cross-sectional area equivalence principle

A cross-sectional area equivalence principle [Pan, Wang, Ma et al. (2014)] is commonly used to build simple equivalent models of launch vehicles for load calculation, control, dynamic analysis, etc. It is easy to establish an equivalent beam model with annular cross-section according to the geometry of the stiffened cylindrical shell through this principle. The core idea of the principle lies in the equivalence of the longitudinal ribs. In launch vehicles, the number of longitudinal ribs is usually 40 to 120, which can be regarded as uniformly distributed. The longitudinal ribs influence the bending, torsional and longitudinal stiffness of the stiffened cylindrical shell through their contributions to the moments of area of the shell. The effects of circumferential ribs are usually not considered. The shape and eccentricity of the longitudinal rib has negligible influence on the equivalence accuracy of this principle [Pan, Wang, Ma et al. (2014)] because the diameter of the stiffened cylindrical shell is much larger than the cross-section size of the ribs. For convenience, it is assumed that all the longitudinal ribs are identical. The cross-section shape of the ribs is circular with a radius r_{rib}, and the axis of the ribs locates in

the shell skin [Pan, Wang, Ma et al. (2014)]. The cross-sectional area, A_{rib}, the second moment of area, I_{rib}, and the polar moment of area, J_{rib}, relative to its centre of the longitudinal rib can be easily written as:

$$A_{\mathrm{rib}} = \pi r_{\mathrm{rib}}^2 \tag{1}$$

$$I_{\mathrm{rib}} = \frac{\pi r_{\mathrm{rib}}^4}{4} \tag{2}$$

$$J_{\mathrm{rib}} = 2I_{\mathrm{rib}} = \frac{\pi r_{\mathrm{rib}}^4}{2} \tag{3}$$

The cross-section area of the stiffened cylindrical shell, A_0, can be written as:

$$A_0 = 2\pi r_{\mathrm{skin}} t_{\mathrm{skin}} + \sum_{i=1}^{n} A_i = 2\pi r_{\mathrm{skin}} t_{\mathrm{skin}} + nA_{\mathrm{rib}} \tag{4}$$

where r_{skin} is the average radius of the stiffened cylindrical shell, t_{skin} is the thickness of the shell skin, A_i is the cross-section area of each longitudinal rib, n is the number of the longitudinal ribs.

The thickness of the equivalent annular cross-section beam, t, can be calculated by

$$t = \frac{A_0}{2\pi r_{\mathrm{skin}}} = t_{\mathrm{skin}} + \frac{nA_{\mathrm{rib}}}{2\pi r_{\mathrm{skin}}} = t_{\mathrm{skin}} + t_{\mathrm{rib}} \tag{5}$$

where t_{rib} is the thickness contributed by longitudinal ribs.

The area moment of inertia, I, and the polar moment of area, J, of the equivalent beam can be easily written as:

$$I = \frac{\pi}{4} r_{\mathrm{skin}} t\left(4r_{\mathrm{skin}}^2 + t^2\right) \approx \pi r_{\mathrm{skin}}^3 t \tag{6}$$

and

$$J = 2I = \frac{\pi}{2} r_{\mathrm{skin}} t\left(4r_{\mathrm{skin}}^2 + t^2\right) \approx 2\pi r_{\mathrm{skin}}^3 t \tag{7}$$

In Eqs. (6) and (7), the second-order small quantity t^2 has been neglected. The area moment of inertia, I_0, of the stiffened cylindrical shell can be written as:

$$I_0 = \frac{\pi}{4} r_{\mathrm{skin}} t_{\mathrm{skin}}\left(4r_{\mathrm{skin}}^2 + t_{\mathrm{skin}}^2\right) + n\left(I_{\mathrm{rib}} + \frac{A_{\mathrm{rib}}}{2} r_{\mathrm{skin}}^2\right) \approx \pi r_{\mathrm{skin}}^3 t + nI_{\mathrm{rib}} \tag{8}$$

The polar moment of area of the stiffened cylindrical shell, J_0, is not twice as much as its area moment of inertia [Pan, Wang, Ma et al. (2014)], I_0. And the contribution from the longitudinal ribs to the torsional stiffness of the stiffened cylindrical shell is far less than that from the shell skin, the polar moment of area of the shell, J_0, can be written approximately as:

$$J_0 = \frac{\pi}{2} r_{\mathrm{skin}} t_{\mathrm{skin}}\left(4r_{\mathrm{skin}}^2 + t_{\mathrm{skin}}^2\right) \approx 2\pi r_{\mathrm{skin}}^3 t_{\mathrm{skin}} \tag{9}$$

In Eqs. (8) and (9), the second-order small quantity t_{skin}^2 has been neglected.

From Eqs. (6) and (8), $\frac{I_0}{I}$ can be calculated

$$\frac{I_0}{I} = \frac{\pi r_{\mathrm{skin}}^3 t + nI_{\mathrm{rib}}}{\pi r_{\mathrm{skin}}^3 t} = 1 + \frac{r_{\mathrm{rib}}^2}{2r_{\mathrm{skin}}^2\left(1 + \frac{2r_{\mathrm{skin}} t_{\mathrm{skin}}}{nr_{\mathrm{rib}}^2}\right)} \tag{10}$$

Since r_{skin} is far larger than r_{rib} in launch vehicles, $\frac{I_0}{I}$ equals to 1 approximately, i.e., the area moment of inertia of the equivalent beam is equal to that of the stiffened cylindrical shell approximately.

From Eqs. (7) and (9), $\frac{J_0}{J}$ can be calculated

$$\frac{J_0}{J}=\frac{2\pi r_{\mathrm{skin}}^3 t_{\mathrm{skin}}}{2\pi r_{\mathrm{skin}}^3 t}=\frac{t_{\mathrm{skin}}}{t}=\frac{1}{1+\frac{t_{\mathrm{rib}}}{t_{\mathrm{skin}}}} \tag{11}$$

Since $\frac{t_{\mathrm{rib}}}{t_{\mathrm{skin}}}$ cannot be neglected, the polar moment of area of the equivalent beam is much different from that of the stiffened cylindrical shell, a correction of the polar moment of area of the equivalent beam is needed [Pan, Wang, Ma et al. (2014)], and from Eq. (11), the correction factor, c_{tor}, is given by

$$c_{\mathrm{tor}}=\frac{t_{\mathrm{skin}}}{t} \tag{12}$$

The final polar moment of area of the equivalent beam is

$$J^*=c_{\mathrm{tor}}J=\frac{\pi}{2}r_{\mathrm{skin}}t_{\mathrm{skin}}\left(4r_{\mathrm{skin}}^2+t^2\right)\approx 2\pi r_{\mathrm{skin}}^3 t_{\mathrm{skin}} \tag{13}$$

3 Weighted nodal displacement coupling relationship

There are l nodes. Their coordinates are $\mathbf{d}_i=(x_i,y_i,z_i)^{\mathrm{T}}$, $i=1,2,\ldots,l$, and their displacements are $\mathbf{u}_i=\left(u_{ix},u_{iy},u_{iz}\right)^{\mathrm{T}}$. The weighted nodal displacement coupling relationship is to create a new node, $\mathbf{d}_{\mathrm{c}}=(x_{\mathrm{c}},y_{\mathrm{c}},z_{\mathrm{c}})^{\mathrm{T}}$, and use its displacement, $\mathbf{u}_{\mathrm{c}}=\left(u_{cx},u_{cy},u_{cz}\right)^{\mathrm{T}}$, to represent the displacements of the l nodes.

Firstly, the weighted centre coordinate, $\mathbf{d}_{\mathrm{o}}=(x_{\mathrm{o}},y_{\mathrm{o}},z_{\mathrm{o}})^{\mathrm{T}}$, of the l nodes and its displacement, $\mathbf{u}_{\mathrm{o}}=\left(u_{ox},u_{oy},u_{oz}\right)^{\mathrm{T}}$, are calculated as:

$$q_{\mathrm{o}}=\frac{\sum_{i=1}^{l}w_{iq}q_i}{\sum_{i=1}^{l}w_{iq}},\ u_{oq}=\frac{\sum_{i=1}^{l}w_{iq}u_{iq}}{\sum_{i=1}^{l}w_{iq}},\ (q=x,y,z) \tag{14}$$

where, w_{ix}, w_{iy}, w_{iz} are weighting coefficients for each degree of freedom of each node, usually taken as 1.

Then, assuming that there are no relative motions between the l nodes, a rigid region is formed. According to the rigid body motion relationship, the rigid-body displacement of node i, $\mathbf{u}_i^*=\left(u_{ix}^*,u_{iy}^*,u_{iz}^*\right)^{\mathrm{T}}$, can be written as:

$$\mathbf{u}_i^*=\mathbf{u}_{\mathrm{o}}+\boldsymbol{\alpha}\mathbf{r}_i \tag{15}$$

where

$$\boldsymbol{\alpha}=\begin{bmatrix}0 & -\alpha_z & \alpha_y\\ \alpha_z & 0 & -\alpha_x\\ -\alpha_y & \alpha_x & 0\end{bmatrix},\ \mathbf{r}_i=\mathbf{d}_i-\mathbf{d}_{\mathrm{o}} \tag{16}$$

α_x, α_y, and α_z are the angles of rotation about x-, y- and z-axis of the rigid region. They can be determined by minimizing the modulus, $|\boldsymbol{\varepsilon}|$, of vector $\boldsymbol{\varepsilon} = \left(\varepsilon_x, \varepsilon_y, \varepsilon_z\right)^{\mathrm{T}}$ of the error functions of $\mathbf{u}_i^*$ and $\mathbf{u}_i$ using the least-squares method

$$\varepsilon_q = \sum_{i=1}^{l} w_{iq}\left(u_{iq}^* - u_{iq}\right)^2,\ (q = x, y, z) \tag{17}$$

Finally, the displacement vector of node $\mathbf{d}_{\mathrm{c}}$ can be determined

$$\mathbf{u}_{\mathrm{c}} = \mathbf{u}_{\mathrm{o}} + \boldsymbol{\alpha}(\mathbf{d}_{\mathrm{c}} - \mathbf{d}_{\mathrm{o}}) \tag{18}$$

The specific steps of using this relationship to transform the displacements of the nodes in the fine FEM model of a stiffened cylindrical shell to the node displacements of the equivalent beam model are introduced in Section 5.2 in detail.

4 Iterative model updating method using modal data

Modal data include natural frequencies and mode shapes of a structure, which are the common kinds of targets used in model updating. The iterative model updating method using modal data [Friswell and Mottershead (1995)] needs to select some physical and geometric parameters of the structure as design parameters and analyse their sensitivities. Normally, the natural frequencies and mode shapes vary with the design parameters nonlinearly, so it is necessary to linearize them by truncating the first-order Taylor expansion [Mottershead, Link and Friswell (2011)]. Using $\mathbf{z}_{\mathrm{obj}}$ to represent the vector consisting of the interested natural frequencies and mode shapes, $\mathbf{z}$ to represent the vector consisting of the corresponding finite element analysis results, $\boldsymbol{\theta}$ to represent the vector consisting of the design parameters, the relationship between them is defined as

$$\mathbf{z}_{\mathrm{obj}} \approx \mathbf{z}_m + \mathbf{S}(\boldsymbol{\theta}_{m+1} - \boldsymbol{\theta}_m) \tag{19}$$

where, subscript m represents the mth iteration, $\mathbf{S}$ is sensitivity matrix consisting of the first derivatives of the natural frequencies, $\omega_k (k = 1,2,\cdots,H)$, and the mode shapes, $\boldsymbol{\phi}_k$, with respect to the design parameters, $\theta_j (j = 1,2,\cdots)$.

For an eigenvalue problem

$$\mathbf{K}\boldsymbol{\phi}_k = \omega_k^2 \mathbf{M}\boldsymbol{\phi}_k \tag{20}$$

where $\mathbf{M}$ and $\mathbf{K}$ are the mass matrix and stiffness matrix of the structure. The expression of the first derivative of the natural frequency, ω_k, is [Friswell and Mottershead (1995)]

$$\frac{\partial \omega_k}{\partial \theta_j} = \frac{1}{2\omega_k} \boldsymbol{\phi}_k^{\mathrm{T}} \left[\frac{\partial \mathbf{K}}{\partial \theta_j} - \omega_k^2 \frac{\partial \mathbf{M}}{\partial \theta_j}\right] \boldsymbol{\phi}_k \tag{21}$$

The complete eigenvector derivative is given by a linear combination of all H eigenvectors of the structure [Friswell and Mottershead (1995)]

$$\frac{\partial \boldsymbol{\phi}_k}{\partial \theta_j} = \sum_{h=1}^{H} c_h \boldsymbol{\phi}_h = \mathbf{v}_k + c_k \boldsymbol{\phi}_k \tag{22}$$

the eigenvector, $\boldsymbol{\phi}_k$, follows mass normalization equation

$$\boldsymbol{\phi}_k^{\mathrm{T}} \mathbf{M} \boldsymbol{\phi}_k = 1 \tag{23}$$

By differentiating Eq. (23) with respect to θ_j, and combining with Eq. (22), the participation factor, c_k, is obtained

$$c_k = -\boldsymbol{\phi}_k^{\mathrm{T}}\mathbf{M}\mathbf{v}_k - \frac{1}{2}\boldsymbol{\phi}_k^{\mathrm{T}}\frac{\partial \mathbf{M}}{\partial \theta_j}\boldsymbol{\phi}_k \tag{24}$$

A problem arises in the computation of $\mathbf{v}_k$ and a solution is given by Nelson [Friswell and Mottershead (1995)].

Eqs. (21) and (22) are the theoretical formulas for calculating the sensitivities of natural frequencies and mode shapes, and in the practical operation, they are usually calculated approximately by using numerical differentiation method.

By rearranging Eq. (19), the explicit iteration updating relationship of design parameters is obtained

$$\boldsymbol{\theta}_{m+1} = \boldsymbol{\theta}_m + \mathbf{S}^{+}\left(\mathbf{z}_{\mathrm{obj}} - \mathbf{z}_m\right) \tag{25}$$

where $\mathbf{S}^{+}$ is the inverse sensitivity matrix. Since the system of linear algebraic equations in Eq. (19) is often over-determined or under-determined, it cannot be inverted directly. The inverse sensitivity matrix [Friswell and Mottershead (1995)], $\mathbf{S}^{+}$, is calculated as:

$$\mathbf{S}^{+} = \begin{cases} [\mathbf{S}^{\mathrm{T}}\mathbf{S}]^{-1}\mathbf{S}^{\mathrm{T}} & \text{over determined} \\ \mathbf{S}^{-1} & \text{determined} \\ \mathbf{S}^{\mathrm{T}}[\mathbf{S}\mathbf{S}^{\mathrm{T}}]^{-1} & \text{under determined} \end{cases} \tag{26}$$

5 Beam approximation process

In this section, the beam approximation process for dynamic analysis of launch vehicles modelled as stiffened cylindrical shells is presented in detail. Firstly, an initial beam model is established based on the cross-sectional area equivalence principle. Then, a fine FE model of the stiffened cylindrical shell is established and a modal analysis is carried out. Some natural frequencies and mode shapes are selected as the model updating targets, and the mode shapes are translated by using the weighted nodal displacement coupling relationship. Finally, the initial beam model is improved through model updating against the natural frequencies and mode shapes of the fine FE model.

5.1 Initial equivalent beam model

The stiffened cylindrical shell mainly consists of skin, longitudinal ribs and circumferential ribs. Based on the cross-sectional area equivalence principle, the skin and the longitudinal ribs are represented as a beam model with annular cross-section located on the axis of the stiffened cylindrical shell and the circumferential ribs are ignored. In this paper, for the purpose of ensuring that the mass distribution of the beam model is the same as that of the stiffened cylindrical shell along the longitudinal direction, the circumferential ribs are represented as lumped masses applied to the nodes of the beam model. The specific steps are as follows:

a) According to the geometry of the stiffened cylindrical shell, the cross-section area of each longitudinal rib is calculated, and then the thickness of the annular cross-section beam is obtained from Eqs. (4) and (5).

b) Taking the diameter of the shell skin as the diameter, the beam model with annular cross-section is established. The longitudinal locations of the beam nodes correspond to those of the circumferential ribs of the shell.

c) According to the material properties of the stiffened cylindrical shell, the mass of each circumferential rib is calculated and applied to the corresponding node of the beam model as a lumped mass.

The material properties of the initial equivalent beam model are set in step b) according to those of the stiffened cylindrical shell. If the materials of the skin and the longitudinal ribs are different, the material properties of the beam model need to be estimated. It has to be noted that the mass distribution of the initial beam model should be as close as possible to the longitudinal mass distribution of the stiffened cylindrical shell. Other material attributes can be roughly selected.

5.2 Model updating targets

The fine FE model of the stiffened cylindrical shell is established, and modified if there are experimental data. Then, a modal analysis of the fine FE model is implemented. Some natural frequencies and mode shapes are selected as the model updating targets. The natural frequencies can be directly used to improve the equivalent beam model. While the mode shapes cannot, because of the nodes of the fine FE model of the shell and the equivalent beam model are not one-to-one correspondence. The weighted nodal displacement coupling relationship is used to transform the nodal displacements between the two models. For a mode shape, the specific steps are as follows:

a) The nodes on the plane located the circumferential rib are selected and the node of equivalent beam model corresponding to the circumferential rib is selected.

b) According to Eqs. (14) to (18), the displacements of the nodes on the plane are represented by the displacement of the node of the beam model.

c) Steps a) and b) are repeated several times until the displacements of the nodes on the planes located the circumferential ribs are all represented by the displacements of the nodes of the beam model.

5.3 Model updating

Since the mass distribution of the beam model has been settled in Section 5.1, it is considered to be exact. A problem may occur during model updating, because of the great difference between the fine FE model and the equivalent beam model. If all the design parameters are directly used for model updating at the same time, they can easily converge to incorrect values, for example, the Young's modulus, E, may become negative. And it is hard to give the exact ranges of the design parameters directly. Having a pre-model updating procedure before the proper model updating to shift design parameters close to the convergent values can ease this problem. In pre-model updating, based on the sensitivity analysis and practical experiences, the area moments of inertia, I_1, and, I_2, in two directions, the polar moment of area, J_{p}, and Young's modulus, E, of the beam element are selected as design parameters. There are no range limitations of the design parameters, and, generally, they are converged to reasonable values. Usually, using these four design parameters the bending and torsional modes of the equivalent beam model can be corrected. The axial modes are sensitive to the cross-sectional area, A, and Young's modulus, E, of the beam, and these two parameters are closely related to the

mass distribution and the bending modes of the beam model. So, in order to improve the axial modes, some linear spring elements are introduced between each pair of adjacent nodes of the equivalent beam model, and their stiffness, k, is selected as design parameter. All the design parameters of each element in the beam model are same. Those five design parameters are determined by using the natural frequencies of the first and the second bending modes in the two normal directions, the first torsional and the first axial modes of the fine FE model of the shell structure (totally six modes). The flow chart of pre-model updating is shown in Fig. 2, which includes five steps:

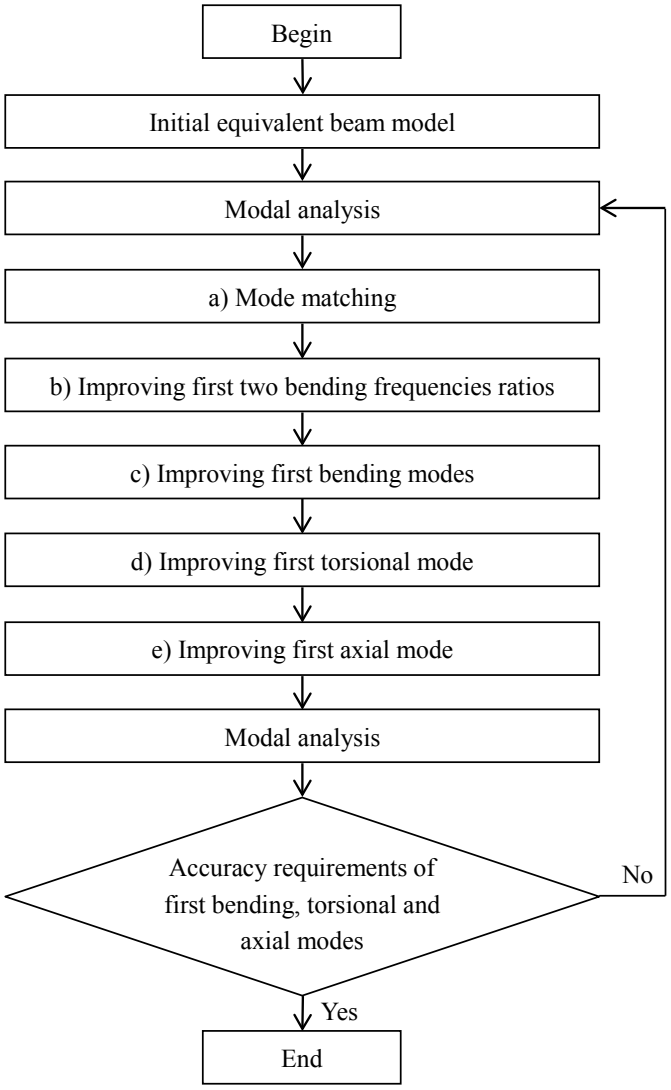

Figure 2: The flow chart of pre-model updating

a) A modal analysis is taken to the initial equivalent beam model. The modal assurance criteria (MAC) values [Friswell and Mottershead (1995)] between the mode shapes of the beam model and those of the stiffened shell are calculated. The MAC value between the ith mode shape of the beam model and the jth targeted mode is calculated from

$$\mathrm{MAC}_{ij} = \frac{\left|\boldsymbol{\varphi}_i^{\mathrm{T}}\boldsymbol{\psi}_j\right|^2}{\left(\boldsymbol{\varphi}_i^{\mathrm{T}}\boldsymbol{\varphi}_i\right)\left(\boldsymbol{\psi}_j^{\mathrm{T}}\boldsymbol{\psi}_j\right)} \tag{27}$$

The closer the MAC value is to 1, the higher correlation of the two mode shapes is in. For each targeted mode shape, one mode shape of the beam model is identified that brings the MAC value of the two closest to 1. Then such two modes are paired. This process is called mode matching.

b) The ratio of the natural frequencies of the first two bending modes, β, is improved.

$$\beta = \frac{\omega_{\mathrm{b1}}}{\omega_{\mathrm{b2}}} \tag{28}$$

where ω_{b1} and ω_{b2} are the natural frequencies of the first and second bending modes. The area moments of inertia, I_1, and, I_2, are selected as the design parameters to improve β. In addition, for the case in which the frequencies of the first bending modes in two perpendicular out-of-plane directions are different, the same design parameters are taken to improve the ratio of the two frequencies, γ.

$$\gamma = \frac{\omega_{\mathrm{b1}}^{(1)}}{\omega_{\mathrm{b1}}^{(2)}} \tag{29}$$

where the superscripts (1) and (2) represent two bending directions.

c) The first bending modes are improved. The Young's modulus, E, is selected as the design parameter.

d) Now the first torsional mode is improved. The polar moment of area, J_{p}, is selected as the design parameter.

e) Afterwards, the first axial mode is improved. The stiffness of the spring elements, k, is selected as the design parameter, and the initial value come from

$$k_0 = \frac{(E_0 - \hat{E})A}{L} \tag{30}$$

where, E_0 is the initial Young's modulus value of the beam element, $\hat{E}$ is the Young's modulus value after step c), A and L are the cross-sectional area and the length of the beam element.

The above steps are repeated several times until the frequencies of the afore-mentioned six modes of the equivalent beam model match the corresponding frequency of the fine FE model to the required accuracy. The values of design parameters after pre-model updating are quite different from those of the initial beam model, but the bending rigidity, torsional rigidity and tensile stiffness of the beam model before and after pre-model updating have not much, as shown in Section 6.1, which is expected and indirectly reflects that the finial equivalent beam model shows similar global static properties as the original model. And, it should be noted that, because of the beam approximation method presented in this paper is focused on the global dynamic performances of the original

model, the equivalent beam model can reflect only the global static properties of the original model.

On this basis, the proper updating can be carried out to consider the higher frequencies and other quantities of interest. The ranges of the design parameters can be given if needed. For a simple stiffened cylindrical shell, its equivalent beam model can be obtained in good accuracy just by pre-model updating and this is presented in the next section.

6 Numerical examples

To verify the effectiveness of this method, two examples are given in this section. One is stiffened cylindrical shells with a circular cross-section. The other is a composite structure of stiffened cylindrical shells. The fine FE models and the equivalent beam models of the two examples are built in ANSYS. In the fine FE models, SHELL181 and BEAM188 elements are used to build the skins and ribs of the stiffened cylindrical shells. The material properties are Young's modulus of 200 GPa, Poisson's ratio of 0.33, density of 7850 kg/m^3. The equivalent beam models are established by using MASS21, BEAM188, and COMBIN14 elements and improved in the authors' MATLAB codes. The modal analyses of the finite element models in the paper are made in ANSYS using block Lanczos method.

6.1 Stiffened cylindrical shell of circular cross-section

The stiffened cylindrical shell of circular cross-section is 50 m long and 5 m in diameter. Its skin thickness is 0.01 m. 8 circular longitudinal ribs with a diameter of 0.15 m and 11 circular circumferential ribs with a diameter of 0.6 m are distributed uniformly. There are totally 3200 SHELL181 elements, 1152 BEAM188 elements and 3232 nodes in the fine FEM model. A normal mode analysis of the fine FEM model is taken and frequencies and modes below 100 Hz are extracted. The beam model is established to reflect the first two bending, torsional and axial modes of the stiffened cylindrical shell, totally 6 modes, and the errors of the natural frequencies should be less than 2%, and the MAC values should be greater than 0.95. There are totally 10 BEAM188 elements, 10 COMBIN14 elements and 11 nodes in the beam model. The parameter values of the normal mode analysis of the equivalent beam model are the same as those of the fine FEM model of the shell. The values of design parameters before and after model updating are shown in Tab. 1. The calculation results of the bending rigidity, torsional rigidity and tensile stiffness are given in Tab. 2. The shear modulus, G, is calculated by

$$G = \frac{E}{2(1+\mu)} \tag{31}$$

where μ is Poisson's ratio. The tensile stiffness, K, of the beam model is calculated by

$$K = \frac{EA}{L} + k \tag{32}$$

The torsional rigidity between brackets in Tab. 2 is calculated from the modified polar moment of area calculated by Eq. (13). In Tab. 1, the values of design parameters after pre-model updating are quite different from those of the initial beam model. And in Tab. 2, it is shown that the bending rigidity, torsional rigidity and tensile stiffness of the beam model before and after pre-model updating are not changed a lot. This indirectly reflects

that the finial equivalent beam model shows similar static properties as the original model.

Table 1: The values of design parameters before and after pre-model updating

Name	Initial beam model	After pre-model updating
Area moment of inertia I_1(m^4)	0.93019	3.85737
Area moment of inertia I_2(m^4)	0.93019	3.85737
Polar moment of area J_p(m^4)	1.86038	4.10773
Young's modulus E(Pa)	2.00000×10^{11}	4.86976×10^{10}
Spring stiffness k(N/m)	0	9.07265×10^{9}

Table 2: The bending rigidity, torsional rigidity and tensile stiffness of the beam model before and after pre-model updating

Name	Initial beam model	After pre-model updating
Bending rigidity EI_1(N·m^2)	1.86038×10^{11}	1.87845×10^{11}
Bending rigidity EI_2(N·m^2)	1.86038×10^{11}	1.87845×10^{11}
Torsional rigidity GJ_p(N·m^2)	1.39878×10^{11} (7.38155×10^{10})	7.52017×10^{10}
Tensile stiffness K(N/m)	1.19381×10^{10}	1.19794×10^{10}

The results of the modal analysis are shown in Tabs. 3 and 4. The natural frequencies of the beam model after model updating and the fine FEM model under 100 Hz are calculated and are compared in Tab. 4. The relative error between the kth natural frequency of the equivalent beam model, ω_k, and the target, $\omega_{\mathrm{obj},k}$, is defined as:

$$\varepsilon_k = \frac{|\omega_k - \omega_{\mathrm{obj},k}|}{\omega_{\mathrm{obj},k}} \times 100\% \tag{33}$$

Table 3: The modal analysis results of circular cross-section stiffened cylindrical shell

Mode shape	Fine FEM model	Initial beam model			After pre-model updating		
	Natural freq. $\frac{\omega_{\mathrm{obj}}}{2\pi}$/ Hz	Natural freq. $\frac{\omega_{\mathrm{init}}}{2\pi}$/ Hz	Error ε/%	MAC	Natural freq. $\frac{\omega_{\mathrm{beam}}}{2\pi}$/ Hz	Error ε/%	MAC
1st bending	5.08693	5.30697	4.33	1.00	5.08685	0.00	1.00
2nd bending	12.0315	13.4858	12.09	1.00	12.0321	0.00	1.00
1st torsional	10.4780	17.9169	71.00	1.00	10.4780	0.00	1.00
2nd torsional	20.8148	35.9476	72.70	1.00	21.1493	1.61	0.99
1st axial	23.5534	23.5036	0.21	1.00	23.5531	0.00	1.00
2nd axial	46.7567	46.7197	0.08	1.00	46.8182	0.13	1.00

Table 4: The under 100 Hz natural freq. of the beam and the fine FEM model

Mode shape	Equivalent beam model $\frac{\omega_{\text{beam}}}{2\pi}$/ Hz	Fine FEM model $\frac{\omega_{\text{obj}}}{2\pi}$/ Hz	Error ε/%	MAC
1st bending	5.08685	5.08693	0.00	1.00
1st torsional	10.4780	10.4780	0.00	1.00
2nd bending	12.0321	12.0315	0.00	1.00
3rd bending	19.8983	19.8237	0.38	1.00
2nd torsional	21.1493	20.8148	1.61	0.99
1st axial	23.5531	23.5534	0.00	1.00
4th bending	27.6192	27.3096	1.13	1.00
3rd torsional	32.1963	30.8625	4.32	0.98
Higher bending	34.7504	33.4403	3.92	1.00
Higher bending	40.9770	41.6252	1.56	1.00
4th torsional	43.7677	40.4604	8.17	0.96
Higher bending	46.1146	46.3863	0.59	1.00
2nd axial	46.8182	46.7567	0.13	1.00
Higher bending	49.9529	50.1041	0.30	1.00
Higher bending	52.3582	52.4540	0.18	1.00
Higher torsional	55.9241	49.4290	13.14	0.93
Higher mode	61.4747	68.5988	10.39	1.00
Higher mode	65.8044	70.6128	6.81	0.98
Higher torsional	68.5282	57.5659	19.04	0.91
3rd axial	69.4816	69.2395	0.35	1.00
Higher bending	75.4475	80.1641	5.88	0.95
Higher torsional	81.0534	64.6387	25.39	0.88
Higher mode	89.5765	93.6324	4.33	0.92
4th axial	91.1822	90.6218	0.62	1.00
Higher torsional	92.3630	70.2221	31.53	0.88

As it is shown in Tab. 3, after pre-model updating, the first two bending, torsional and axial natural frequencies of the stiffened cylindrical shell predicted by the equivalent beam model are already in good agreement with the original structure, and thus the subsequent proper model updating is not necessary except for accurate prediction of higher frequencies if needed. And in Tab. 4, the relative errors of the natural frequencies of the first four bending, axial modes and the first three torsional modes are below 5%. It is shown that, for a simple stiffened cylindrical shell, its equivalent beam model can be obtained in good accuracy just by pre-model updating.

6.2 Composite structure of stiffened cylindrical shells

As shown in Fig. 3, a composite structure of stiffened cylindrical shells with a total height of 50 m and width of 13 m is presented. The shell stage 1, stage 2 and the dome-shaped fairing located at the centre comprise the central stage. The diameters of them are 5 m, and the heights of them are 25 m, 20 m and 5 m, respectively. Four boosters with a

diameter of 3.5 m and a height of 25 m are distributed around the centre. The distances between boosters and stage 1 are 0.5 m and the connections are modelled by BEAM188 elements. Since the model in this example is mainly to verify the beam approximation method, the connection between the booster and stage 1 is simplified as a beam. There are two nodes built on the axes of each booster and stage 1. Each node is connected to the nearest circumferential rib by rigid beam elements. The beams for connecting the boosters with stage 1 are built between the two corresponding nodes of the boosters and stage 1. The skin thicknesses of the central stage and each booster are 0.01 m. The distributions of the longitudinal and circumferential ribs are shown in Fig. 3. There are 8 longitudinal ribs and 10 circumferential ribs in the central stage and each booster. The cross-section of the longitudinal and circumferential ribs of the central stage is 0.15 m and 0.6 m in diameter, respectively. The cross-section of the longitudinal and circumferential ribs of each booster is 0.1 m and 0.4 m in diameter, respectively. That of the connection beams is 0.5 m in diameter. There are totally 9504 SHELL181 elements, 1776 BEAM188 elements, 192 rigid beam elements (96 elements each group to construct rigid region) and 9555 nodes (2 nodes with no mass for constructing rigid region) in the fine FEM model of the stage included stage 1, stage 2 and fairing. There are totally 3264 SHELL181 elements, 1064 BEAM188 elements, 128 rigid beam elements (64 elements each group to construct rigid region) and 3299 nodes (2 nodes with no mass for constructing rigid region) in the fine FEM model of each booster. Each connection is modelled by a BEAM188 element. A normal mode analysis of the fine FEM model of the whole structure is made and the first 16th non-rigid-body modes are extracted.

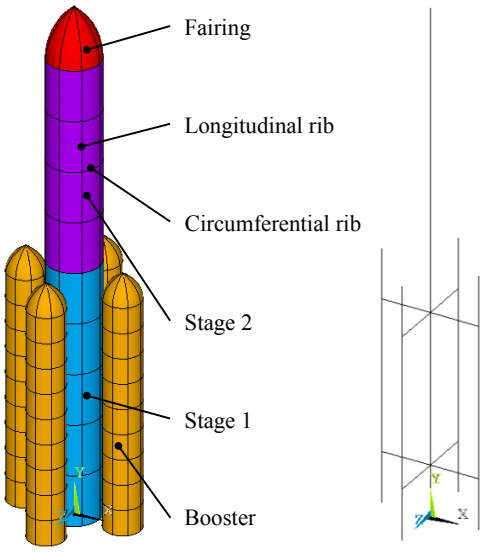

Figure 3: The sketch of the composite structure of stiffened cylindrical shells and its equivalent beam model

The equivalent beam model is established based on a substructure technique. The components of the composite structure are reduced respectively at first, and then

assembled together. The model reduction process of each component is similar to that of the previous example. The first two bending and the first torsional and axial modes of each component are selected as the model updating targets for the corresponding equivalent beam model. The selected design parameters of each equivalent beam model are the same as the previous example. The fairing and the head of the boosters are located at the end of the cylindrical structures, their contributions to the stiffness of the composite structure are small, and only their masses should be made reasonably equivalent. It has to be noted that stage 1 and the boosters are connected, and hence their equivalent beam models should not only reflect the free modal characteristics of the structure without the nodes on the axes and the rigid beam elements, but also the constrained modal characteristics. The results of the design parameters after model updating with the targets of the free modal characteristics are the bases of the model updating with the targets of the constrained modal characteristics. In this example, the fixed constraints are imposed on the two nodes built on the axes of each booster and stage 1, and the results of the design parameters after the model updating with the targets of the constrained modal characteristics are selected as the final structure parameters. And the connections between stage 1 and the boosters should be improved after assembly. There are totally 10 BEAM188 elements, 10 COMBIN14 elements and 11 nodes in the equivalent beam model of each booster and the whole stage. The parameter values of the normal mode analysis of the equivalent beam model of the whole structure are the same as those of the fine FEM model. The modal analysis results are shown in Tab. 5, and the mode shapes are given in Fig. 4.

Table 5: The modal analysis results of the composite stiffened cylindrical shells

Mode No.	Fine FEM model	Equivalent beam model		
	Natural freq. $\frac{\omega_{\text{obj}}}{2\pi}$/Hz	Natural freq. $\frac{\omega_{\text{beam}}}{2\pi}$/Hz	Error ε/%	MAC
1	2.23412	2.22368	0.47	1.00
2	2.51765	2.50270	0.59	0.99
3	2.51765	2.50270	0.59	0.99
4	3.96638	3.96429	0.05	1.00
5	3.96638	3.96429	0.05	1.00
6	6.67768	6.81119	2.00	1.00
7	8.14362	8.14422	0.01	1.00
8	8.67321	8.67464	0.02	0.99
9	8.67321	8.67464	0.02	0.99
10	9.58198	9.58669	0.05	1.00
11	10.7373	10.7320	0.05	1.00
12	10.7373	10.7320	0.05	1.00
13	11.2967	11.0753	1.96	1.00
14	13.1984	13.2035	0.04	1.00
15	13.2337	13.1830	0.38	1.00
16	13.2337	13.1830	0.38	1.00

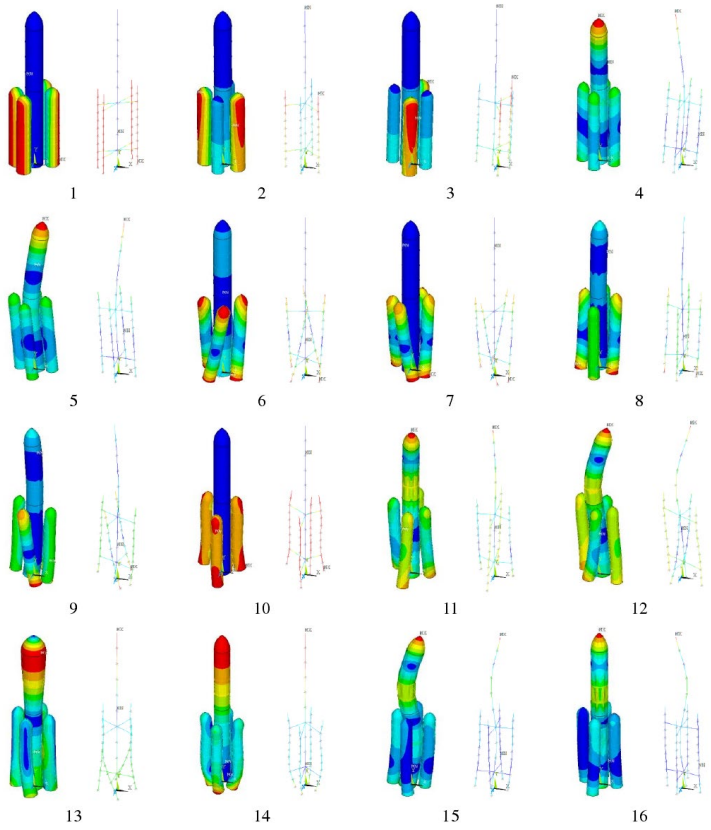

Figure 4: The mode shapes of the composite structure of stiffened cylindrical shells

In this example, only the first several modes of each component have been modified, and as shown in Tab. 5, the largest relative error among the first 16 natural frequencies of the whole structure is 2% (for the 6th natural frequency). And in Fig. 4, the mode shapes of the equivalent beam model are similar to those of the fine FEM model.

For a composite structure of stiffened cylindrical shells, like a launch vehicle, the lower modes are usually most concerned and they are made up from the lower modes of individual components. The construction of the equivalent beam model for each component that captures the lower modes of the original structure can provide an accurate reduced model for the whole composite structure.

7 Conclusions

An equivalent beam model for dynamic analysis of launch vehicles modelled as stiffened cylindrical shells is successfully established. Model updating method is applied to improve the beam model of the stiffened cylindrical shells. Three aspects of this work lead to its success. In establishing the initial equivalent beam model, some improvements are made to the cross-sectional area equivalence principle. The mass distribution of the initial equivalent beam model is the same as that of the stiffened cylindrical shell along the longitudinal direction. In comparing the mode shapes, by introducing the weighted

nodal displacement coupling relationship, the relation between the mode shapes of the detailed FE model of the stiffened cylindrical shell and its equivalent beam model is constructed. In model updating, the whole process is split into two procedures, which helps prevent the design parameters from converging to incorrect values.

The method proposed in this paper is an improvement of the method proposed by Pan et al. [Pan, Wang, Ma et al. (2014)]. There are three main advantages of the improved method compared with the common methods.

a) The physical meaning of the equivalent beam model is clear. It is easy to build an intuitive FE model of the equivalent beam using conventional beam elements in commercial software. The improved method and the method proposed by Pan et al. both have clear physical meanings. The whole model reduction process does not depend on the experience of the analyst, and the high-accuracy equivalent beam models of the stiffened cylindrical shells can be established by follow some simple steps.

b) Compared with the method proposed by Pan et al., the improved method can take into account the influences of the circumferential ribs of the stiffened cylindrical shells, so the mass distributions of the beam models are much closer to those of the shells along the longitudinal direction. And the model updating against the modal analysis results of the shells is given to the beam models, so they can have a higher accuracy.

c) The method proposed by Pan et al. has a limitation of applicability. A good accuracy can be obtained only if the cross-sectional moment of area of the equivalent beam is close to that of the original structure. It means that the method proposed by Pan et al. is more suitable for establishing the equivalent beam models of the stiffened cylindrical shells with large diameter of the shell skins, small cross-section size and densely distributed of the longitudinal ribs, and few circumferential ribs. The improved method is not subjected to these limitations.

It should be pointed out that although the proposed method improves the accuracy of the equivalent beam model through model updating, it needs to establish a fine FEM model of the original structure, which undoubtedly increases some extra work of the model reduction process compared with the method proposed by Pan et al.

A real launch vehicle consists of several kinds of stiffened cylindrical shells which need to be classified at first. The stiffened cylindrical shells which constitute the main structures of the launch vehicle need to be reduced separately. If the length of the stiffened cylindrical shell is short, it should be conceptually grouped with a few other stiffened cylindrical shells so that all together the grouped shells are long enough to be modelled as a beam. Generally, when the slenderness ratio of a stiffened cylindrical shell is more than 10, its global dynamic behaviour becomes similar to that of a beam. For the other stiffened cylindrical shells which are very short and mainly used for connection. The equivalent beam models of them need to be updated together with the equivalent beam models of the stiffened cylindrical shells connected by them. After all the stiffened cylindrical shells are reduced properly, they are assembled together to determine the connections between the different stages and boosters.

For applying this method to the general situation, the basic ideas are the same. Firstly, the mass distribution of the equivalent beam model should be the same as that of the

stiffened cylindrical shell along the longitudinal direction, which is relatively easy to achieve mathematically. The next step is the adjustment of the stiffness distribution, which is the difficult part in beam model equivalence. If the stiffened cylindrical shell is very complex along the longitudinal direction, it needs to be conceptually divided into several simple segments, and many design parameters have to be selected to get the equivalent model, which will bring many problems. This method is more suitable for establishing the equivalent beam model of the structure composed of several simple slender stiffened cylindrical shells.

For further development of this method, one action is introducing additional degrees of freedom to enrich the representativeness of the equivalent beam model, to improve the accuracy and to expand the application, so that it can be used to describe accurately such structures as stiffened cylindrical shells with large openings on their side walls. The other is the application of model updating method combined with weighted nodal displacement coupling relationship. Such an improved method will have the ability to establish the equivalent models of other kinds of large and complex structures.

Acknowledgment: The authors are grateful for support under grants from the National Natural Science Foundation of China (11672060, 11672052).

Conflicts of Interest: The authors declare that they have no conflicts of interest to report regarding the present study.

References

Afonso, S. M. B.; Lyra, P. R. M.; Albuquerque, T. M. M.; Motta, R. S. (2010): Structural analysis and optimization in the framework of reduced-basis method. *Structural and Multidisciplinary Optimization*, vol. 40, no. 1-6, pp. 177-199.

Benfield, W. A.; Hruda, R. F. (1971): Vibration analysis of structures by component mode substitution. *AIAA Journal*, vol. 9, no. 7, pp. 1255-1261.

Box, G. E. P.; Wilson, K. B. (1951): On the experimental attainment of optimum conditions. *Journal of the Royal Statistical Society: Series B (Methodological)*, vol. 13, no. 1, pp. 1-45.

Cai, Y. W.; Xu, L.; Cheng, G. D. (2014): Novel numerical implementation of asymptotic homogenization method for periodic plate structures. *International Journal of Solids and Structures*, vol. 51, no. 1, pp. 284-292.

Cheng, G. D.; Cai, Y. W.; Xu, L. (2013): Novel implementation of homogenization method to predict effective properties of periodic materials. *Acta Mechanica Sinica*, vol. 29, no. 4, pp. 550-556.

Cheng, G. D.; Wang, W. S. (2014): Fast dynamic analysis of complicated beam-type structure based on reduced super beam model. *AIAA Journal*, vol. 52, no. 5, pp. 952-963.

Cortex, C.; Vapnik, V. (1995): Support-vector networks. *Machine Learning*, vol. 20, no. 3, pp. 273-297.

Craig, R. R.; Bampton, M. (1968): Coupling of substructures for dynamic analysis.

AIAA Journal, vol. 6, no. 7, pp. 1313-1319.

Davila, C. G.; Bisagni, C.; Rose, C. A. (2015): *Effect of Buckling Modes on the Fatigue Life and Damage Tolerance of Stiffened Structure*.

https://ntrs.nasa.gov/archive/nasa/casi.ntrs.nasa.gov/20150006850.pdf.

Friswell, M. I.; Garvey, S. D.; Penny, J. E. T. (1995): Model reduction using dynamic and Iterated IRS techniques. *Journal of Sound and Vibration*, vol. 186, no. 2, pp. 311-323.

Friswell, M. I.; Mottershead, J. E. (1995): *Finite Element Model Updating in Structural Dynamics*. Kluwer Academic Publishers, Netherlands.

Grimes, P. J.; Mc Tigue, L. D.; Riley, G. F.; Tilden, D. I. (1970): *Advancements In Structural Dynamic Technology Resulting from Saturn 5 Programs, Volume 1*. https://ntrs.nasa.gov/archive/nasa/casi.ntrs.nasa.gov/19700019695.pdf.

Guyan, R. J. (1965): Reduction of stiffness and mass matrices. *AIAA Journal*, vol. 3, no. 2, pp. 380.

Hajela, P.; Berke, L. (1992): Neural networks in structural analysis and design: an overview. *Computing Systems in Engineering*, vol. 3, no. 1, pp. 525-538.

Hao, P.; Wang, B.; Tian, K.; Li, G.; Du, K. et al. (2016): Efficient optimization of cylindrical stiffened shells with reinforced cutouts by curvilinear stiffeners. *AIAA Journal*, vol. 54, no. 4, pp. 1-14.

Hao, P.; Wang, B.; Tian, K.; Li, G.; Sun, Y. et al. (2017): Fast procedure for non-uniform optimum design of stiffened shells under buckling constraint. *Structural and Multidisciplinary Optimization*, vol. 55, no. 4, pp. 1503-1516.

Hilburger, M. W.; Lindell, M. C.; Waters, W. A.; Gardner, N. W. (2017): *Test and Analysis of Buckling-Critical Stiffened Metallic Launch Vehicle Cylinders*.

https://ntrs.nasa.gov/archive/nasa/casi.ntrs.nasa.gov/20190000441.pdf.

Hou, S. N. (1969): *Review of Modal Synthesis Techniques and A New Approach*. https://ntrs.nasa.gov/archive/nasa/casi.ntrs.nasa.gov/19700033203.pdf.

Kaintura, A.; Spina, D.; Couckuyt, I.; Knockaert, L.; Bogaerts, W. et al. (2017): A kriging and stochastic collocation ensemble for uncertainty quantification in engineering applications. *Engineering with Computers*, vol. 33, no. 4, pp. 935-949.

Koutsovasilis, P.; Beitelschmidt, M. (2008): Comparison of model reduction techniques for large mechanical systems. *Multibody System Dynamics*, vol. 20, no. 2, pp. 111-128.

Kuhar, E. J.; Stahle, C. V. (1974): Dynamic transformation method for modal synthesis. *AIAA Journal*, vol. 12, no. 5, pp. 672-678.

Li, Y. W.; Wang, B.; Cheng, G. D. (2017): Frequency analysis of stiffened cylinder based on novel reduced order model. *Astronautical Systems Engineering Technology*, vol. 1, no. 1, pp. 41-48.

Li, Y. W.; Hao, P.; Wang, B.; Tian, K. (2019): A model-reduction method based on proper orthogonal decomposition for stiffened shells. *Acta Mechanica Solida Sinica*, vol. 40, no. 4, pp. 334-341.

Matheron, G. (1963): Principles of geostatistics. *Economic Geology*, vol. 58, no. 8, pp. 1246-1266.

Mottershead, J. E.; Friswell, M. I. (1993): Model updating in structural dynamics: a survey. *Journal of Sound and Vibration*, vol. 167, no. 2, pp. 347-375.

Mottershead, J. E.; Link, M.; Friswell, M. I. (2011): The sensitivity method in finite element model updating: a tutorial. *Mechanical Systems and Signal Processing*, vol. 25, no. 7, pp. 2275-2296.

Nurre, G. S.; Ryan, R. S.; Scofield, H. N.; Sims, J. L. (1984): Dynamics and control of large space structures. *Journal of Guidance Control and Dynamics*, vol. 7, no. 5, pp. 514-526.

Pan, Z. W.; Wang, X. J.; Ma, X. R.; Gu, L. X. (2014): Longitudinal-lateral-torsional integrated modelling based on a beam model for skin-stiffened structure. *Scientia Sinica Technologica*, vol. 44, no. 5, pp. 517-524.

Pinson, L. D. (1970): *Evaluation of A Finite-Element Analysis for Longitudinal Vibrations of Liquid Propellant Launch Vehicle*.
https://ntrs.nasa.gov/archive/nasa/casi.ntrs.nasa.gov/19700020450.pdf.

Samuel, E. R.; Ferranti, F.; Knockaert, L.; Dhaene, T. (2016): A hybrid adaptive sampling algorithm for obtaining reduced order models for systems with frequency dependent state-space matrices. *International Journal of Numerical Modelling-Electronic Networks Devices and Fields*, vol. 29, no. 4, pp. 741-754.

Wang, W. S.; Cheng, G. D.; Li, Q. H. (2013): Fast dynamic performance optimization of complicated beam-type structures based on two new reduced physical models. *Engineering Optimization*, vol. 45, no. 7, pp. 835-850.

Wang, B.; Tian, K.; Hao, P.; Zheng, Y.; Ma, Y. et al. (2016): Numerical-based smeared stiffener method for global buckling analysis of grid-stiffened composite cylindrical shells. *Composite Structures*, vol. 152, pp. 807-815.

Wang, B.; Tian, K.; Zheng, Y. B.; Zhang, K. (2017): A rapid buckling analysis method for large-scale grid-stiffened cylindrical shells. *Acta Aeronautica et Astronautica Sinica*, vol. 38, no. 2, pp. 183-191.

Wang, B.; Li, Y. W.; Hao, P.; Zhou, Y.; Zhao, Y. et al. (2017): Free vibration analysis of beam-type structures based on novel reduced order model. *AIAA Journal*, vol. 55, no. 9, pp. 3143-3152.

Wilson, D. A. (1974): Model reduction for multivariable systems. *International Journal of Control*, vol. 20, no. 1, pp. 57-64.

Wilson, E. L.; Yuan, M. W.; Dickens, J. M. (1982): Dynamic analysis by direct superposition of Ritz vector. *Earthquake Engineering & Structural Dynamics*, vol. 10, no. 6, pp. 813-821.

Zipfel, P. H. (2014): *Modeling and Simulation of Aerospace Vehicle Dynamics*, Third Edition. American Institute of Aeronautics and Astronautics, USA.